JOC The Journal of Organic Chemistry

Article

pubs.acs.org/joc

Understanding α,β-Unsaturated Imine Formation from Amine Additions to α,β-Unsaturated Aldehydes and Ketones: An Analytical and Theoretical Investigation

Adam D. J. Calow,[†] Jorge J. Carbó,*[,‡] Jessica Cid,[‡] Elena Fernández,[‡] and Andrew Whiting*[,†]

[†]Centre for Sustainable Chemical Processes, Department of Chemistry, Science Laboratories, Durham University, South Road, Durham DH1 3LE, U.K.

[‡]Departament Química Física I Inorgànica, University Rovira I Virgili, C/Marcel.lí Domingo s/n, 43007 Tarragona, Spain

Supporting Information

ABSTRACT: A combination of *in situ* IR spectroscopy (ReactIR) and DFT calculations have been used to understand what factors govern the selectivity in the addition of primary amines to α,β-unsaturated aldehydes and ketones, i.e., 1,2- versus 1,4-addition. It has been found that the 1,2-addition products (α,β-unsaturated imines following addition and elimination) usually predominate for most systems. However, exceptions, such as methyl vinyl ketone, selectively give 1,4-addition products. This has been rationalized by DFT calculations that show that major conformational effects are involved, controlled mainly by steric effects of carbonyl substituents, resulting in a model that provides simple and predictable preparation of α,β-unsaturated imines for *in situ* utilization in synthesis.

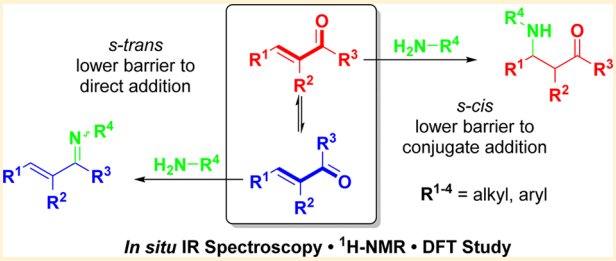

INTRODUCTION

The addition of nucleophiles to conjugated electron-deficient alkenes (e.g., α,β-unsaturated aldehydes, amides, esters, and ketones) is one of the most important C−C and C−heteroatom bond-forming reactions in organic synthesis.[1] However, because of the possibility of conjugate (1,4) versus direct (1,2) addition, a thorough understanding of the factors that govern these competing pathways is required.

We recently developed catalytic asymmetric routes to chiral γ-amino alcohols[2] (Scheme 1), whereby α,β-unsaturated imines **3** were utilized as starting materials by generation *in situ*. The *in situ* generation was absolutely essential to allow this methodology to work on a range of substrates and to give clean products in good yields. However, in the process of preparing these α,β-unsaturated imines **3**,[2] we discovered a lack of kinetic or mechanistic studies regarding the relative 1,2- versus 1,4-addition of primary amines **2** to α,β-unsaturated aldehydes and ketones **1** (enals and enones, respectively). This is surprising given the wealth of studies examining both the aza-Michael[3] reaction and that of classical imine formation (from aldehydes and ketones).[4] Nevertheless, other groups have utilized such imines **3** in synthesis[5−8] and have reported their preparation via aza-Wittig chemistry,[9] simple condensation, and catalytic methods.[10] Herein, we report the use of a combination of *in situ* IR spectroscopy (ReactIR)[11] backed up by NMR studies, and DFT calculations, with the aim of understanding the addition of primary amines **2** to α,β-unsaturated aldehydes and ketones **1** (1,2- vs 1,4-addition) and examine the relative rates of these reactions. Furthermore, we show which 1,2-addition products (i.e., α,β-unsaturated imines **3** following the addition−elimination process) are generated cleanly and in such a way that they can be utilized in synthesis without the need for isolation. This procedure therefore makes a number of α,β-unsaturated imines readily available in an efficient and atom-economic way for further synthetic applications (see Scheme 1).

Scheme 1. *In Situ*-Generated α,β-Unsaturated Imines, Which Are Ideal for Various One-Pot Formation−Functionalization Sequences

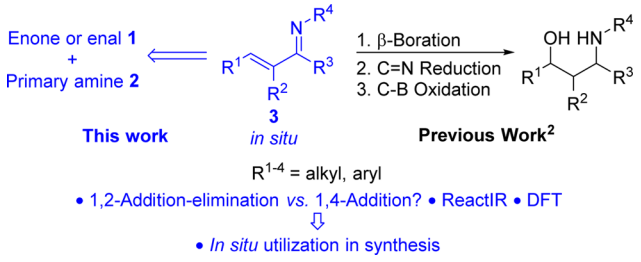

RESULTS AND DISCUSSION

***In Situ* IR Spectroscopy Study.** Initially, we suspected that the addition of a primary amines **2** (R^4-NH_2, where R^4 = alkyl or aryl) to enals or enones **1** would result in a mixture of 1,2-

Received: March 31, 2014
Published: May 5, 2014

   dx.doi.org/10.1021/jo5007366 | J. Org. Chem. 2014, 79, 5163−5172

and 1,4-addition products (i.e., **3** and **4**, respectively). It is typically considered that 1,2-addition products are kinetically preferred and that the 1,4-addition products are thermodynamically preferred because of the reversibility of the 1,2-addition step via facile imine hydrolysis and hemiaminal intermediates.[12] Hence, we initially decided to investigate the addition of benzylamine ($BnNH_2$) **2a** to crotonaldehyde **1a**, methacrolein **1b**, and methyl vinyl ketone **1c**, both with and without 3 Å molecular sieves (3 Å MSs) as drying agents at room temperature (see Table 1).

Table 1. 1,2- or 1,4-Addition of $BnNH_2$ to Crotonaldehyde 1a, Methacrolein 1b, and Methyl Vinyl Ketone 1c[b]

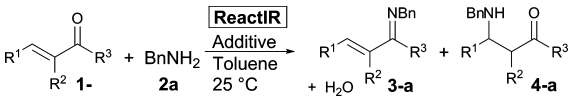

Entry	Substrate **1-**	Additive	Primary Product	Time, t (min)	$I_{C=O\ 1/2}$ (min)
1[a]		3 Å-MS		135	5
2		-		176	5
3[a]		3 Å-MS		80	11
4		-		444	85
5[a]		3 Å-MS		85	6
6		-		82	14

[a]3 Å MSs oven-dried at 250 °C for >48 h prior to use. [b]Enone or enal **1** (2.0 mmol) added to a stirred mixture of toluene (8 mL) and 3 Å MSs (oven-dried at 250 °C for >48 h) at 25 °C. Amine (2.0 mmol) added and monitored by ReactIR.

To our surprise, we observed either exclusive 1,2-addition (entries 1−4, Table 1) or 1,4-addition (entries 4 and 5, Table 1) irrespective of whether 3 Å MSs were present in the reaction mixture. However, it should be noted that in the case of methacrolein **1b**, the reaction time was longer than that of the reaction in which 3 Å MSs were employed (the role of the molecular sieves will be discussed later, *vide infra*), leading to the 1,2-addition product as clearly demonstrated by ReactIR (see Figure 1a−c for typical ReactIR data). More important, however, was the observation that seemingly no 1,4-addition products formed. 1,2-Addition could be clearly deduced (as shown by Figure 1a−c) because the reaction profiles clearly showed the loss of the C═O absorption at 1703 cm^{-1} for methacrolein **1b** and the concomitant appearance of **3ba** shown graphically by the C═N absorption at 1622 cm^{-1}. Figure 1b shows the IR spectrum between 1820 and 1580 cm^{-1} for the reaction of methacrolein **1b** with $BnNH_2$ **2a** and an overlay of three spectra at different time intervals (0, 10, and 80 min). This shows that there is total loss of the starting C═O stretch and that this is synchronized with the rise of the C═N (both asymmetric and symmetric) stretches, and importantly, there is no observable 1,4-addition product at higher wavenumbers. Finally, Figure 1c shows the ReactIR output, showing the intensity of the stretch (arbitrary units, AU) versus wavenumber (cm^{-1}) over time.

Interestingly, in the case of methyl vinyl ketone **1c**, no 1,2-addition product **3** was observed (entries 5 and 6, Table 1); only 1,4-addition took place, as shown in panels a and b of Figure 2, even when 3 Å MSs were employed. This suggests that 1,4-addition product **4** is kinetically preferred by ketone **1c**. An alternative explanation is that there is a facile and rapid hydrolysis of the imine (by the water generated from the condensation), thus releasing amine **2a** to proceed to conduct the 1,4-addition, i.e., under thermodynamic control. However, this is unlikely given that an imine intermediate was not observed in the case of the reaction of **1a** and **1b**, especially when no 3 Å MSs were used. This is particularly clear from ReactIR studies, as shown in Figure 2a, which shows the rapid loss of the carbonyl stretch of **1c** (i.e., C═O stretch at 1686 cm^{-1}) and the concomitant gain of the secondary amine **4ca**, where the carbonyl stretch appears at a higher wavenumber (1719 cm^{-1}). The 1,4-addition product **4ca** was also found to be consumed after 30 min, which is likely due to further addition of secondary amine **4ca** to unsaturated ketone **1c**, which is demonstrated by the loss of the C═O stretch at 1719 cm^{-1}. Indeed, when studied in parallel with the ReactIR (Figure 2b), further 1,4-addition is clearly observed by the appearance of the C═O stretch at a higher wavelength (1719 cm^{-1}).

To validate the ReactIR results listed in Table 1, we conducted parallel *in situ* NMR experiments in d_8-toluene for the reactions between crotonaldehyde **1a**, methacrolein **1b**, and methyl vinyl ketone **1c** and benzylamine **2a**, both with and without 3 Å MSs. Some of these results are shown in Table 2 and Figure 3a−c, which portrays results that are complementary to those reported in Table 1 and Figures 1a−c and 2a,b (additional experimental data are reported in the Supporting Information).

The results shown in Table 2 broadly corroborate the findings obtained from the ReactIR studies (*vide supra*). Some enones, such as methyl vinyl ketone **1c**, undergo exclusive 1,4-addtion with primary amines, indicating that the 1,4-addition pathway is kinetically preferred. In contrast, methacrolein and crotonaldehyde undergo exclusive 1,2-addition, suggesting that in these cases the kinetic preference is for the 1,2-addition route. Moreover, the presence of 3 Å MSs does not change the reaction outcome; however, in some cases, the presence of 3 Å MSs appears to drive the reaction closer to completion, as one might expect, presumably because of the removal of water pushing the condensation equilibrium. This is exemplified by methacrolein **1b** (entries 3 and 4, Table 2).

Next, the role of amine **2** and solvent in selectivity and rates of reaction with the three previously investigated carbonyl compounds (**1a−c**) were investigated using benzylamine **2a**, aniline **2b**, and *n*-butylamine **2c** in nonpolar (toluene) and polar (acetonitrile) solvents, as outlined in Tables 3 and 4.

From Tables 3 and 4, the first thing to note is that all the reactions proceeded to completion in <24 h when the reactions were conducted in toluene, whereas in acetonitrile, some reactions took >24 h (i.e., when using $PhNH_2$ **2b**). However, irrespective of whether the solvent was nonpolar (toluene) or polar (acetonitrile), the reactions proceeded to give the same selectivity that one would expect from Table 1; i.e., **1a** and **1b** undergo 1,2-addition irrespective of the amine, and **1c** reacts exclusively in a 1,4-fashion with all the amines. In particular, the reaction between $PhNH_2$ **2b** and crotonaldehyde **1a** is particularly interesting because of the rapid consumption of carbonyl compound **1a** and the formation of imine **3ab**. Further, the C═O peak intensity dropped 50% after only 9 min (entry 1, Table 3), yet the reaction did not reach completion until approximately 6 h later (see Figure 4), which suggests that the reaction involves rapid hemiaminal formation, followed by a slower dehydration to provide the imine (*vide infra*).

dx.doi.org/10.1021/jo5007366 | J. Org. Chem. 2014, 79, 5163−5172

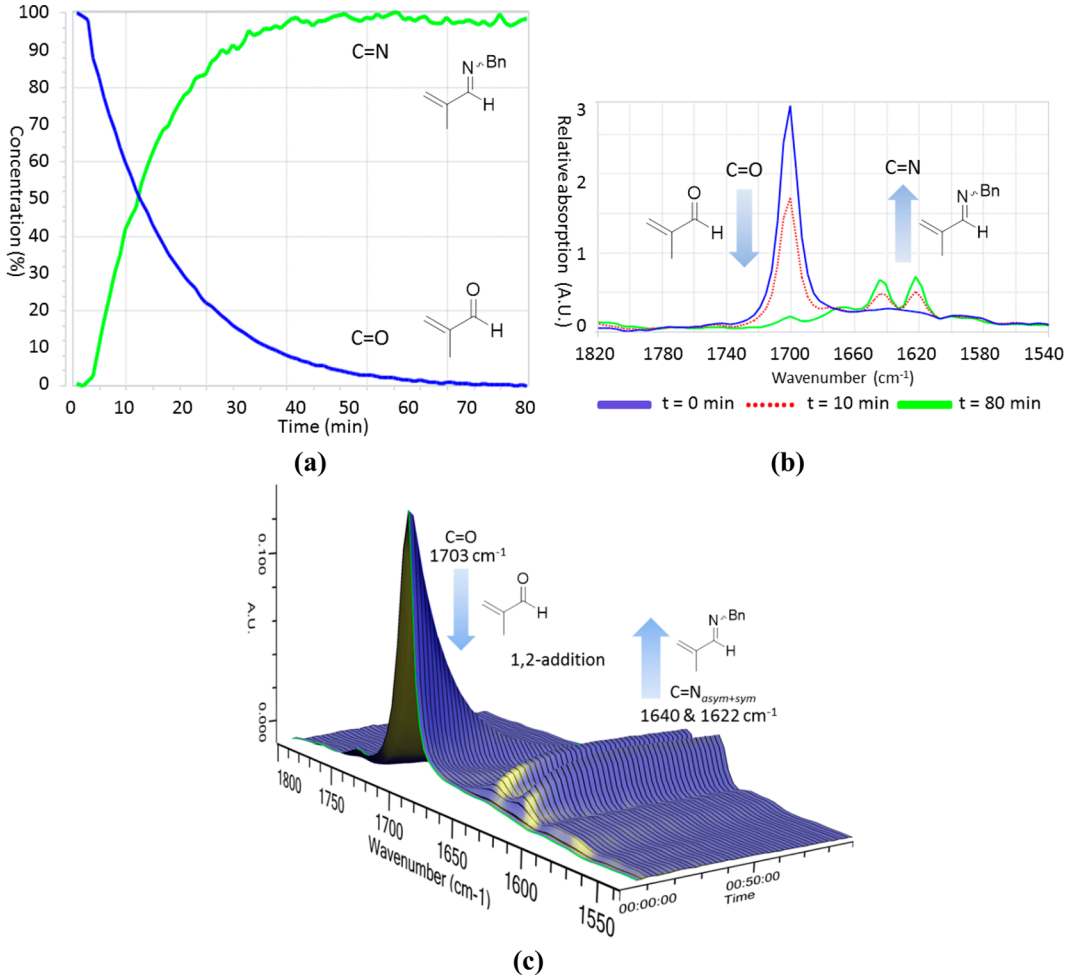

Figure 1. Data from entry 3 of Table 1. (a) Reaction profile showing the loss of **1b** (1703 cm^{-1}) and the concomitant gain of **3ba** (1622 cm^{-1}), 1,2-addtion. (b) Superimposed IR spectra at 0, 10, and 80 min, showing the loss of C═O **1b** (1703 cm^{-1}) and the gain of the $C{=}N_{asym+sym}$ stretches for **3ba** (at 1640 and 1622 cm^{-1}, respectively). (c) ReactIR showing the reaction profile over time (one sample per minute).

Furthermore, imine formation appears to mirror the loss of the enal or enone, suggesting that the rate-determining step is the addition of the amine, and not the collapse of the hemiaminal intermediate (Scheme 2), as determined by *in situ* IR spectroscopy. This is consistent with previous kinetic studies of imine formation in weakly acidic (3 Å MSs) to neutral media.[13] Indeed, when such reactions were performed at acidic pH, the rate-limiting step was found to be the addition of the amine to the corresponding carbonyl, because of competing amine protonation under the acidic conditions.[4] Moreover, acidic conditions aid the dehydration of the hemiaminal intermediate and formation of the imine. In contrast, at basic pH, the rate-determining step switched to collapse of the hemiaminal intermediate.[13]

Next, three cyclic enones, cyclopentenone **1d**, cyclohexenone **1e**, and 3-methyl-2-cyclohexenone **1f**, were examined in their reaction with $BnNH_2$ **2a** and $PhNH_2$ **2b** in toluene (see Table 5). It was assumed, given the exclusive 1,4-addition observed in the case of **1c**, that the increased ring strain of the *α,β*-unsaturated conjugated system results in the same 1,4-addition pathway that is observed with methyl vinyl ketone **1c**. However, to our surprise, 1,2-addition was observed in all cases, though these reactions required >24 h to reach completion. The C═O stretch intensities dropped to 50% (for both cyclopentenone and cyclohexenone) again surprisingly quickly, given the relatively long reaction times, especially in the cases involving the reaction with $BnNH_2$ **2a** (see Figure 5). In particular, 3-methyl-2-cyclohexenone was significantly less reactive with the reaction reaching only 35% conversion to the *α,β*-unsaturated imine after 24 h (see the Supporting Information for IR spectral and *in situ* NMR validation for species **1d**).

We continued our investigation by examining other acyclic enones and enals, looking at the effects of substituents on the C═C bond (i.e., *α,β*-disubstituted enals vs *β*-substituted enals). Hence, cinnamaldehyde **1g** and *α*-methyl-cinnamaldehyde **1h** were compared with the methyl-substituted analogues, crotonaldehyde **1a** and tiglic aldehyde **1i**. In both the latter cases, the *β*-substituted enals reacted significantly faster with $BnNH_2$ **2a** and $PhNH_2$ **2b**. Remarkably, the reaction between cinnamaldehyde **1g** and $BnNH_2$ **2a** was complete in <10 min, with 50% being consumed in approximately 1 min, as shown in the three superimposed IR spectra at 0, 1, and 9 min in Figure 6.

Theoretical Study of the Selectivity in Amine Addition to *α,β*-Unsaturated Aldehydes and Ketones. To understand the origin of the observed selectivity in the addition of amines to the enals and enones, DFT calculations (B3LYP functional) were conducted on representative substrates (i.e., crotonaldehyde **1a**, methyl vinyl ketone **1c**, cyclopentenone **1d**, and pentenone **1j**) using $MeNH_2$ as a

dx.doi.org/10.1021/jo5007366 | J. Org. Chem. 2014, 79, 5163−5172

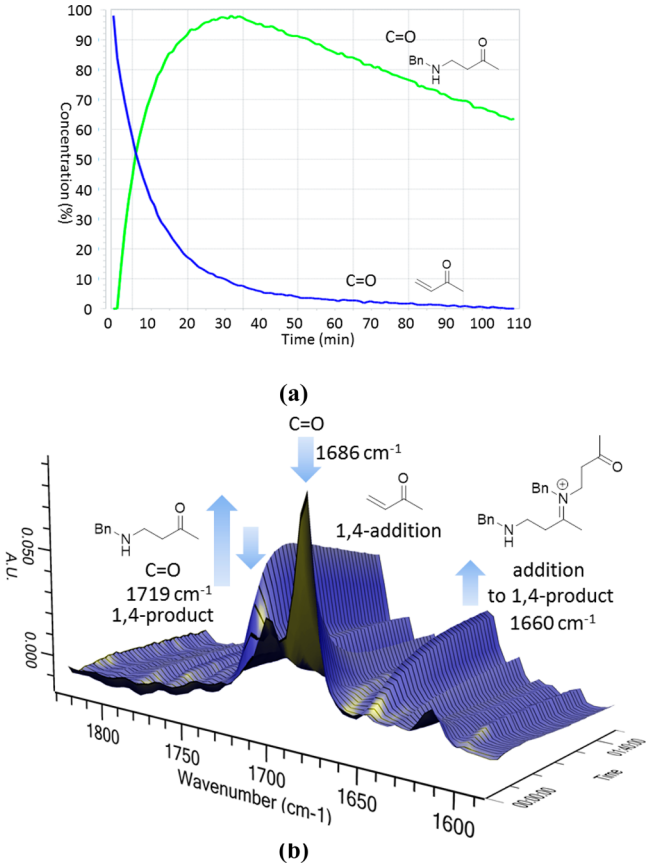

Figure 2. Data from entry 5 of Table 1. (a) Reaction profile showing the rapid loss of **1c** (1686 cm^{-1}) and the concomitant gain of **4ca** (1719 cm^{-1}), followed by the loss of **4ca** (1719 cm^{-1}), consistent with 1,4-addition, with further self-addition of species **4ca** (1660 cm^{-1}). (b) ReactIR graphical output showing the reaction profile over time (one sample per minute).

Table 2. ^{1}H NMR Study of Imine Formation between Carbonyl Compounds 1 and Benzylamine 2a for Comparison with the Results Reported in Table 1[a]

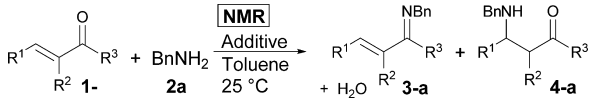

Entry	Substrate **1-**	Additive	Time (min)	Conversion (%) **3-a**	Conversion (%) **4-a**
1	 **1a**	3 Å-MS	310	**3aa** (90)	0
2		-	360	**3aa** (90)	0
3	 **1b**	3 Å-MS	1320	**3ba** (86)	0
4		-	1320	**3ba** (67)	0
5	 **1c**	3 Å-MS	140	0	**4ca** (>99)
6		-	140	0	**4ca** (>99)

[a]Enal or enone **1** (0.18 mmol) added to an NMR tube (Norell Standard Series 5 mm × 178 mm NMR tubes) in d_8-toluene (0.7 mL) with and without 3 Å MSs (filled 0.7−0.8 mm up the tube, MSs oven-dried at 250 °C for >48 h prior to use), flushed with Ar and sealed. After acquisition of the first spectrum, amine **2** (0.18 mmol) added and the next spectrum acquired in <5 min. Subsequent ^{1}H NMR spectra recorded over time with intermittent shaking to aid mixing.

model of a simple primary alkylamine. These calculations indicated that the kinetic preference for the 1,2- versus 1,4-addition pathway depends on the conformational effects operating upon the α,β-unsaturated aldehydes and ketones. When the C=C and C=O bonds are *s-trans* to each other, the 1,2-addition pathway shows lower energy barriers, and in contrast, when they are *s-cis*, the 1,4-addition pathway is preferred (see Table 7 and the Supporting Information for additional comments). Indeed, one should note literature examples that suggest that the stereochemistry involved in the addition of crotyl magnesium chloride to enones is also notably dependent upon the enone conformation.[14]

The predominance for 1,2- over 1,4-addition in the *s-trans* conformation can be explained from the relative energy of the acceptor π^* orbitals.[15] The origin of this effect is due to the fact that energies of the $\pi^*_{C=O}$ orbitals are lower than those of the $\pi^*_{C=C}$ orbitals, suggesting that the electrophilic carbon of the carbonyl group is more reactive than that of the C=C double bond in the *s-trans* conformation. Indeed, for *s-trans* conformers, a linear correlation between the computed energy barriers and the energies of the $\pi^*_{C=O}$ and $\pi^*_{C=C}$ orbitals was observed (see Figure 8). In contrast, when *s-cis* conformers are considered, no correlation between the activation barriers and the energies of the π antibonding orbitals is observed.

In the *s-cis* conformation, the energy barriers for the 1,4-addition pathway [$\Delta E^{\ddagger}(1,4)$] are lowered significantly (~10 kcal mol^{-1}), with respect to those of the *s-trans* forms (see Table 7). Analogously, calculations have shown that the *s-cis* conformation of α,β-unsaturated aldehydes is more reactive toward the addition of dienes.[16] Houk et al. attributed the higher reactivity to the greater electrophilicity of the *s-cis* conformer and also suggested that secondary orbital interactions between the carbonyl and the diene play a key role in controlling stereoselectivity.[16b] Herein, the NBO analysis shows that the reactivity is not consistent with the lower energy of the $\pi^*_{C=C}$ orbitals. Instead, we find a clear correlation with a greater intramolecular $n(C_\alpha) \rightarrow \pi^*_{C=O}$ interaction in the transition state (see Table 7). The developing negative charge at the α-carbon is better delocalized through the $\pi^*_{C=O}$ orbitals when the C=O and (reacting) C=C bonds are *s-cis*. For example, in the 1,4-addition, the transition state of methyl vinyl ketone **1c**, the NBO $n(C_\alpha) \rightarrow \pi^*_{C=O}$ interaction energies (68 and 75 kcal mol^{-1}) correlate with energy barriers of 37.4 and 27.1 kcal mol^{-1} for *s-trans* and *s-cis*, respectively. Indeed, the HOMOs of the transition states have a strong contribution of this interaction, that is, a bonding combination of the p orbitals of the C_α atom and the π^* orbitals of the C=O moiety (see Figure 9). It is important to note that in this TS, the axis of the forming C−H bond is bent toward the C=O moiety in the *s-cis* form, whereas it is bent toward the C(O)-Me in the *s-trans* form, generating two different stereoconfigurations (see Figure 10). In summary, the different balance between electronic effects on going from the *s-trans* to the *s-cis* conformers results in reversing the relative reactivity of the C=C and C=O functional groups.

For crotonaldehyde **1a**, the *s-trans* conformation is thermodynamically favored over the *s-cis* conformation by 1.3 kcal mol^{-1}, thereby selectively leading to the kinetically preferred 1,2-addition imine product **3**. Our computed relative stabilities agree with the results of the high-level calculations[17] and experiments,[18] in which the *s-trans* conformers are favored by 2.1 and 1.7 kcal mol^{-1}, respectively. In addition, vibrational spectroscopic studies showed that the *s-cis* conformation only

dx.doi.org/10.1021/jo5007366 | J. Org. Chem. 2014, 79, 5163−5172

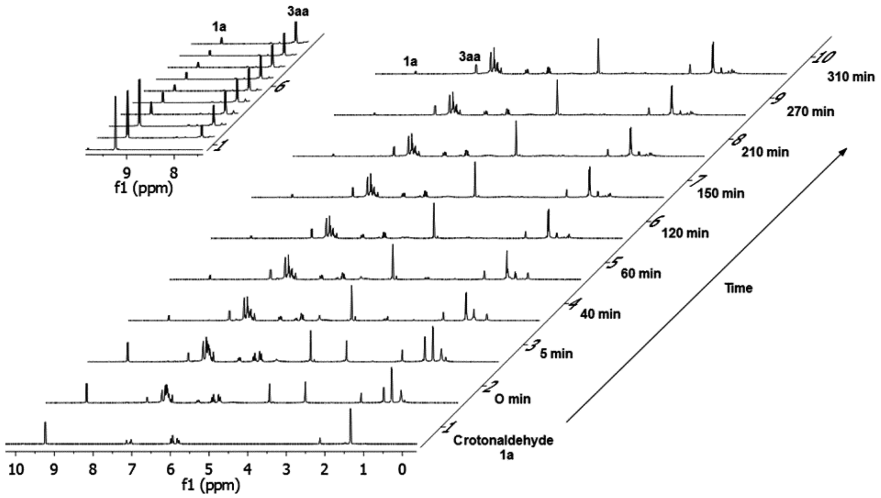

(a)

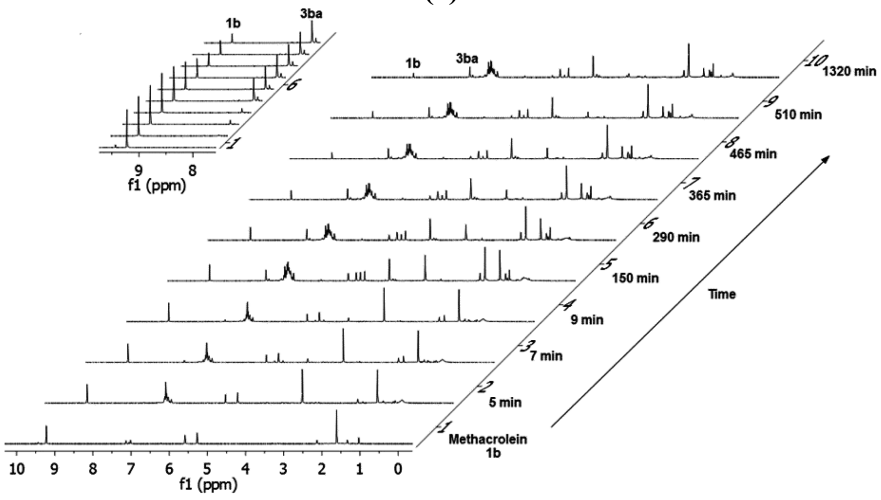

(b)

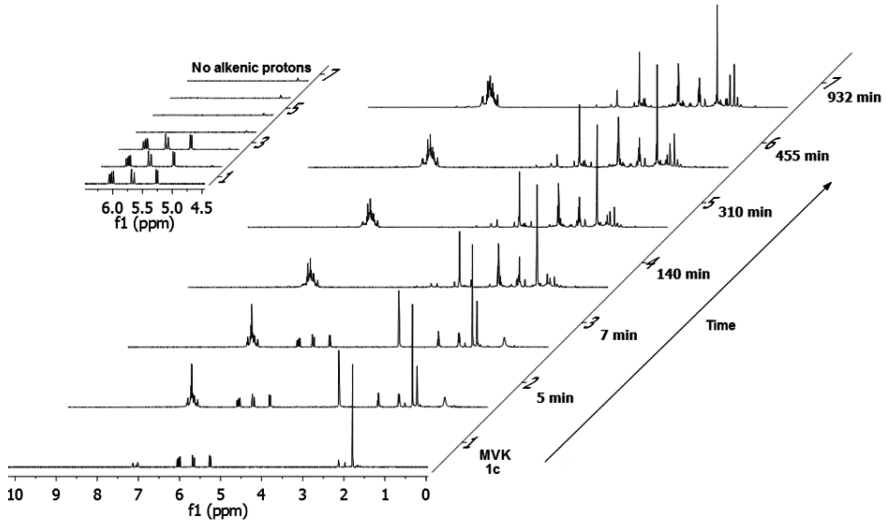

(c)

Figure 3. Real-time ^{1}H NMR experiments showing the reaction between **1a**, **2a**, and **3a** and **2a**, as shown in Table 2: (a) entry 1, (b) entry 3, and (c) entry 5. It should be noted that the reactions appear to be slightly longer when they are conducted under the NMR experimental conditions compared to those employed for the ReactIR experiments. This can be exemplified by comparing the reaction of crotonaldehyde **1a** and benzylamine **2a** in the presence of 3 Å MSs. When monitored by ReactIR, the reaction takes approximately 2.3 h (entry 1, Table 1), whereas in the NMR tube, the reaction takes 5.2 h (entry 1, Table 2) to proceed to near completion. This is useful to know especially in the context of our past experience with using such *in situ*-generated imines directly for further reaction[2] and is likely due to the different mixing (mass transfer) in the NMR tube compared to an efficiently stirred flask used for the ReactIR experiments. In fact, this is an additional advantage of ReactIR in following such reactions over NMR because ReactIR can be conducted directly in the same reaction vessel one would use for further reactions, and on any desired scale.

dx.doi.org/10.1021/jo5007366 | J. Org. Chem. 2014, 79, 5163−5172

Table 3. Probing the Effects of Amine Nucleophilicity in Toluene[a]

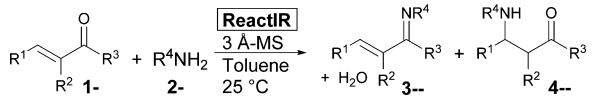

entry	substrate	amine	primary product	time t (min)	$I_{C=O1/2}$ (min)
1	**1a**	$PhNH_2$ **2b**	**3ab**	365	9
2	**1a**	$BnNH_2$ **2a**	**3aa**	135	5
3	**1a**	$nBuNH_2$ **2c**	**3ac**	96	5
4	**1b**	$PhNH_2$ **2b**	**3bb**	632	16
5	**1b**	$BnNH_2$ **2a**	**3ba**	80	11
6	**1b**	$nBuNH_2$ **2c**	**3ba**	87	10
7	**1c**	$PhNH_2$ **2b**	**4cb**	601	50
8	**1c**	$BnNH_2$ **2a**	**4ca**	85	6
9	**1c**	$nBuNH_2$ **2c**	**4cc**	55	3

[a]Standard conditions as reported in the footnote a of Table 1.

Table 4. Probing the Effects of Amine Nucleophilicity in Acetonitrile[a]

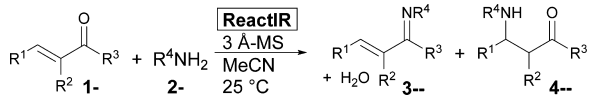

entry	substrate	amine	primary product	time t (min)	$I_{C=O1/2}$ (min)
1	**1a**	$PhNH_2$ **2b**	**3ab**	>1440	57
2	**1a**	$BnNH_2$ **2a**	**3aa**	178	5
3	**1a**	$nBuNH_2$ **2c**	**3ac**	296	4
4	**1b**	$PhNH_2$ **2b**	**3bb**	>1440	42
5	**1b**	$BnNH_2$ **2a**	**3ba**	174	14
6	**1b**	$nBuNH_2$ **2c**	**3ba**	145	12
7	**1c**	$PhNH_2$ **2b**	**4cb**	>1440	474
8	**1c**	$BnNH_2$ **2a**	**4ca**	84	9
9	**1c**	$nBuNH_2$ **2c**	**4cc**	46	3

[a]Standard conditions (except where acetonitrile was used) as reported in footnote a of Table 1.

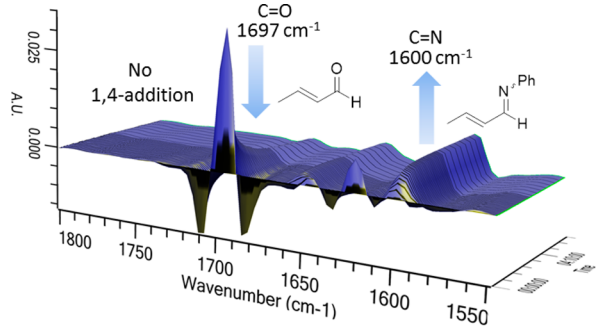

Figure 4. Graphical output of entry 1 of Table 3 showing the rapid loss of the C═O (1697 cm^{-1}) stretch for **1a** and the rise of the C═N (1600 cm^{-1}) stretch of **3ab** upon addition of the soft nucleophile **2b**. A processing second-derivative baseline function is applied, and negative peaks are a product of this processing.

existed in fluid phases,[18] indicating that only the *s-trans* reaction pathway is operative. For the aliphatic ketones **1c** and **1j**, the additional alkyl group most likely induces steric repulsion with the double bond, destabilizing the *s-trans* conformer, which results in a shift in the equilibrium toward the *s-cis* conformer, which becomes more stable by 0.3 and 0.7 kcal mol^{-1} for **1c** and **1j**, respectively. In the case of **1c**, spectroscopic studies revealed that both the *s-cis* and *s-trans* conformations existed,[19] with the energy difference between them reduced to <1 kcal mol^{-1}.[19b] Thus, the reaction is likely to proceed through the lowest-energy transition states available and that means the *s-cis* pathway. These systems of course contrast with the cyclic enones. Because they can adopt only the *s-trans* conformation, the kinetically preferred reaction pathway becomes the 1,2-addition process. Although the energy difference for cyclopentenone **1d** is quite small, it follows the same trend as the other *s-trans* conformer substrates.

Scheme 2. Steps Involved in Imine Formation

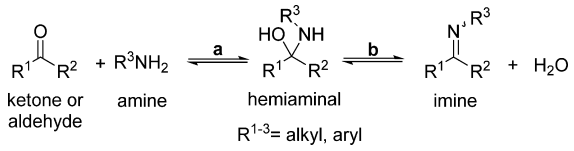

Table 5. Cyclic Enones: 1,2- versus 1,4-Addition with Primary Amines[b]

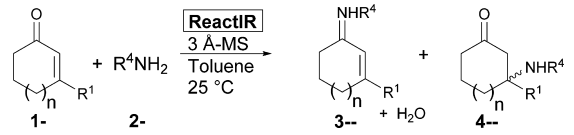

Entry	Substrate **1-**	Amine **2-**	Primary Product	Time, t (h)	$I_{C=O\ 1/2}$ (h)
1	**1d**	$PhNH_2$ **2b**	**3db**	>24	17.4
2	**1d**	$BnNH_2$ **2a**	**3da**	>24	4.0
3	**1e**	$PhNH_2$ **2b**	**3eb**	>>24	7.4
4	**1e**	$BnNH_2$ **2a**	**3ea**	>24	3.5
5	**1f**	$PhNH_2$ **2b**	**3fb**	>>24	-[a]
6	**1f**	$BnNH_2$ **2a**	**3fa**	>24	18.8

[a]Peak intensity of 35% after 24 h. [b]Conditions: enone **1** (2.0 mmol) added to a stirring solution of toluene (8 mL) and 3 Å MSs (oven-dried at 250 °C for >48 h prior to use), amine (2.0 mmol) added and the reaction monitored by ReactIR, and the reaction vessel submerged in an oil bath and the temperature maintained at 25 °C.

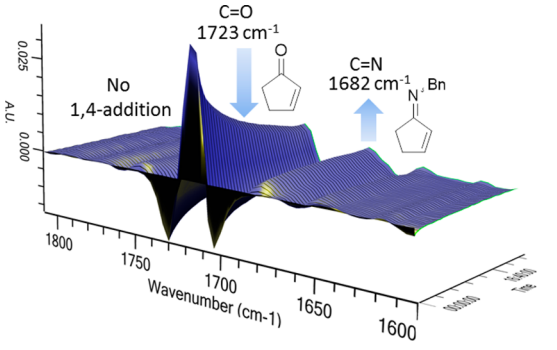

Figure 5. Graphical output of entry 2 of Table 5. Addition of **2a** to **1d** (C═O, 1723 cm^{-1}) results in the slow formation of **3da** (C═N, 1682 cm^{-1}), but no 1,4-addition products are observed. A processing second-derivative baseline function is applied, and negative peaks are a product of this processing.

dx.doi.org/10.1021/jo5007366 | J. Org. Chem. 2014, 79, 5163−5172

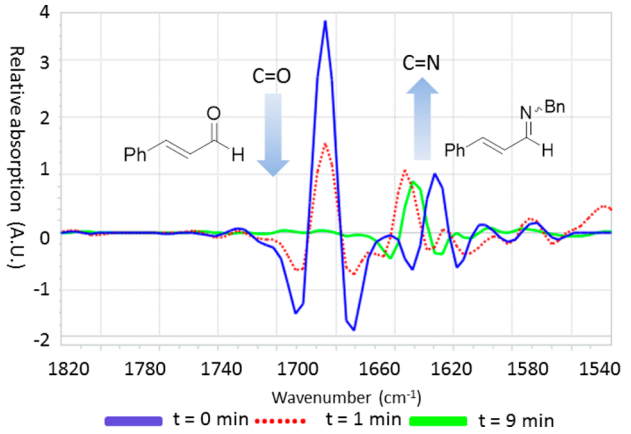

Figure 6. Superimposed IR spectra at 0, 1, and 9 min, showing the loss of **1g** (C═O, 1685 cm^{-1}) and the shift of the C═C stretch in **1g** (from 1630 to 1644 cm^{-1}) upon addition of **2a**. The concomitant gain of the product C═N **3ga** stretch (1641 cm^{-1}) can be observed (entry 2, Table 6). A processing second-derivative baseline function is applied.

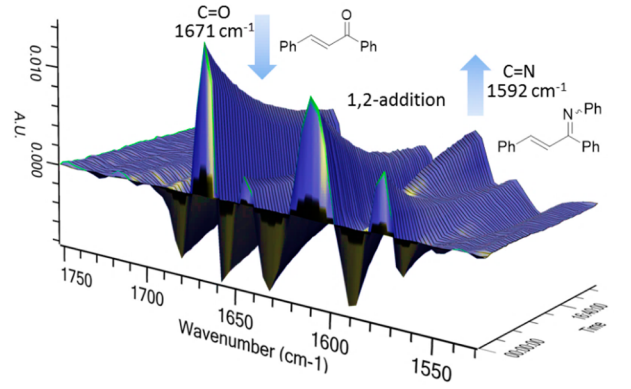

Figure 7. Graphical output of entry 11 of Table 6. Addition of **2b** to **1l** (C═O, 1671 cm^{-1}) results in the slow formation of **3lb** (C═N, 1592 cm^{-1}), but no 1,4-addition products are observed. A processing second-derivative baseline function is applied, and negative peaks are a product of this processing.

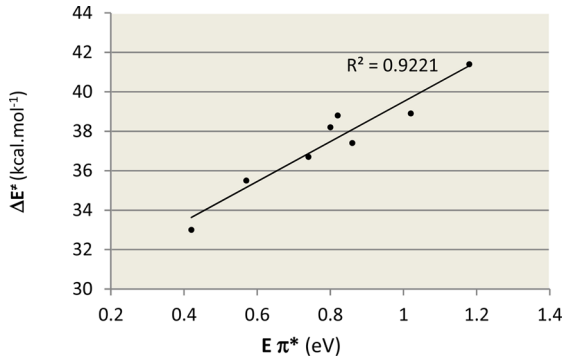

Figure 8. Correlation between the computed energy barriers and the energies of the C═C and C═O π^* orbitals in the *s-trans* isomers.

Via comparison of the different substrates, it was observed that the computed overall energy barriers for the preferred reaction pathways increase in the following order: aliphatic ketone < aldehydes < cyclic ketones. This is in line with experimental results and supports the idea that the nucleophilic amine addition is the rate-determining step under these

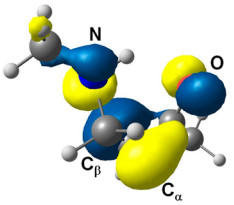

Figure 9. Representation of the $p_{C_\alpha}-\pi^*_{C=O}$ interaction in the HOMO orbital for the transition state of the 1,4-addition in the *s-cis* isomer of **1c**.

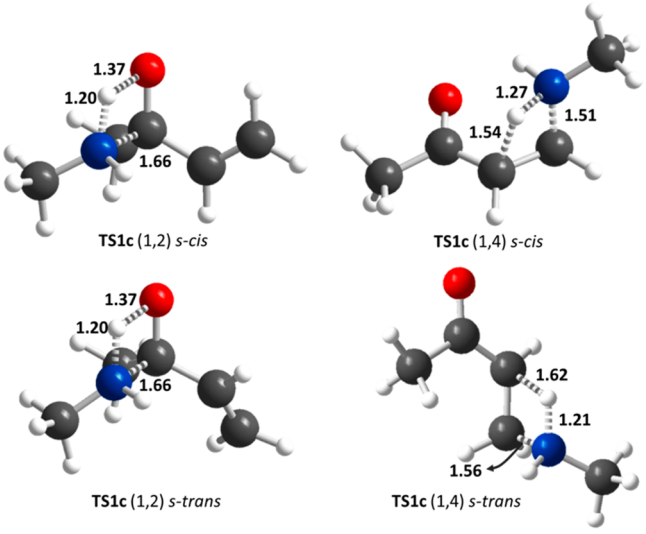

Figure 10. Molecular structures and main geometric parameters of the transition states for the 1,2- and 1,4-addition of $NMeH_2$ to **1c**. Distances in angstroms.

nonacidic conditions. As expected, and in all cases, the 1,4-products are thermodynamically favored over the hemiaminal intermediates resulting from the 1,2-addition mode (see the Supporting Information). Thus, the 1,2-addition product is kinetically controlled, and the 1,4-addition product is observed for methyl vinyl ketone **1c**, which is kinetically preferred as a direct consequence of the change in conformation that occurs.

Upon expanding the scope of the substrates examined by the DFT calculations, we were surprised to find that the other linear enones prefer to give the 1,2-addition products (i.e., **1j**, **1k**, and **1l** in Table 6). This supports the results obtained from the ReactIR and *in situ* ^1H NMR studies (*vide supra* and the Supporting Information). Following from **1c** to **1j**, the calculated barriers showed the same pattern that was previously identified; however, for the 1,4-addition to C═C, they were found to be somewhat higher for **1j** (i.e., by ∼3 kcal mol^{-1}) than for **1c**, as expected for a substrate with an electron-donating substituent on the C═C bond (**1j**).

Summary and Conclusions. The relative reactivity of enones and enals with primary amines has been examined, probing the competitive 1,2- versus 1,4-addition pathway using a combination of *in situ* IR spectroscopy (ReactIR), *in situ* NMR, and DFT calculations. *In situ* IR spectroscopy (ReactIR) revealed that enones and enals undergo either 1,2-addition (to C═O) or 1,4-addition (to C═C) with primary amines (with or without 3 Å MSs). Our results suggest that the formation of *α,β*-unsaturated imines (formed through 1,2-addition to C═O) is under kinetic control for all enals and most enones. However, compounds such as methyl vinyl ketone showed

dx.doi.org/10.1021/jo5007366 | J. Org. Chem. 2014, 79, 5163−5172

Table 6. Probing Substituent Effects of Enals and Enones[b]

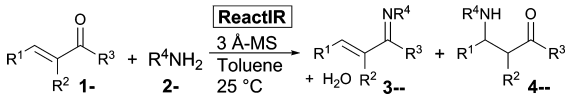

Entry	Substrate 1-	Amine 2-	Primary Product	Time, t (min)	$I_{C=O\ 1/2}$ (min)
1	 1g	$PhNH_2$ **2b**	**3gb**	78	7
2		$BnNH_2$ **2a**	**3ga**	9	1
3	 1h	$PhNH_2$ **2b**	**3hb**	220	25
4		$BnNH_2$ **2a**	**3ha**	202	24
5	 1i	$PhNH_2$ **2b**	**3ib**	545	28
6		$BnNH_2$ **2a**	**3ia**	233	29
7	 1j	$PhNH_2$ **2b**	**3jb**	>1440	-[a]
8		$BnNH_2$ **2a**	**3ja**	>1440	165
9	 1k	$PhNH_2$ **2b**	**3kb**	>1440	139
10		$BnNH_2$ **2a**	**3ka**	>1440	115
11	 1l	$PhNH_2$ **2b**	**3lb**	>1440	517
12		$BnNH_2$ **2a**	**3la**	>1440	108

[a]Peak intensity of 55% after 24 h. [b]Conditions: enone or enal **1** (2 mmol) added to a 25 °C stirred toluene (8 mL) suspension of 3 Å MSs (oven-dried at 250 °C for >48 h prior to use), amine **2** (2 mmol) added, and the reaction monitored by ReactIR.

exclusive 1,4-addition, suggesting that 1,4-addition products (i.e., *β*-amino ketones) are kinetically favored in this case. ReactIR investigations conducted in parallel with a series of *in situ* ^{1}H NMR experiments allowed us to confirm the validity of the observations made by ReactIR, with the exception of those for pentenone **1j**, which showed slow and competing 1,2- versus 1,4-addition (see the Supporting Information). *In situ* methods for the analysis of such substrates and reactions are advantageous because facile hydrolysis, polymerization, and degradation of the sensitive product *α,β*-unsaturated imines are avoided.[20] These problems make isolation of the *α,β*-unsaturated imines problematic, and hence, this highlights the advantages of forming them *in situ* for subsequent transformations. ReactIR is a relatively noninvasive method, with measurements taken *in situ* without causing degradation of air or moisture sensitive intermediates, as exemplified by its use in monitoring low-temperature lithiations.[21]

Stimulated by the data acquired by our ReactIR studies, we turned our attention to seeking theoretical explanations for the observed results. DFT calculations indicated that the selectivities in these addition reactions are governed by conformational and stereoelectonic effects, whereby *s-trans* conformations kinetically favor 1,2-additions and *s-cis* conformations kinetically favor 1,4-additions. Moreover, substitution effects can cause conformational swap-over because of these steric effects.

The rationalization of the interplaying effects involved in preparing unsaturated imines from unsaturated ketones and aldehydes makes the preparation and utilization of the resulting

Table 7. NBO Orbital Energies ($\pi^*_{C=O}$ and $\pi^*_{C=C}$), Energy Barriers ($\Delta E^{\ddagger}$) for the 1,2- and 1,4-Addition, and NBO Second-Order Perturbative Donor−Acceptor Interaction ($n_{C_\alpha} \rightarrow \pi^*_{C=O}$)[a]

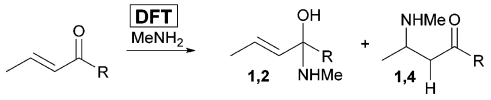

	$\pi^*_{C=O}$	$\Delta E^{\ddagger}(1,2)$	$\pi^*_{C=C}$	$\Delta E^{\ddagger}(1,4)$	$n_{C\alpha}\rightarrow\pi^*_{C=C}$	$\Delta\Delta E^{\ddagger}$
 *s-trans*	**0.42**	**33.0**	**0.82**	**37.4**	**64**	**+4.4**
 *s-cis*	0.41	30.3	1.10	29.0	76	-1.3
 *s-trans*	0.57	35.5	0.86	37.4	68	+1.9
 *s-cis*	**0.63**	**33.4**	**0.98**	**27.1**	**75**	**-6.3**
 *s-trans*	0.74	36.6	1.18	40.1	70	+3.5
 *s-cis*	**0.78**	**34.6**	**1.30**	**30.4**	**75**	**-4.2**
 *s-trans*	**0.80**	**38.2**	**1.02**	**38.9**	**65**	**+0.7**

[a]Orbital energies of $\pi^*_{C=O}$ and $\pi^*_{C=C}$ in electronvolts; and energy barriers and interaction energies in kilocalories per mole. The second-order interaction energies were computed at the trasition state for 1,4-addition.

α,β-unsaturated imines *in situ* more predictable. The clean and selective formation of such imines *in situ* has already proven to be valuable in our hands for reaction with boryl nucleophiles,[2] and it is expected that these results offer the potential for wider applications in synthesis.

EXPERIMENTAL SECTION

General Experimental. All *in situ* IR spectroscopy experiments (ReactIR) were conducted with the following instruments: ReactIR 15 with MCT detector; ConcIRT window of 1900−900 cm^{-1}. Apodization: Happ General. Probe: Prob A DiComp (Diamond) connected via KAgX 9.5 mm × 2 m fiber (silver halide); sampling 2500-650 at 8 cm^{-1} resolution; scan option, auto select, gain 1×. ^{1}H NMR spectra were recorded on a 500 MHz spectrometer, operating at ambient probe temperature unless specified otherwise. Deuterated toluene (d_8-toluene) was used as a solvent for all NMR spectra, unless specified otherwise.

Standard Conditions for ReactIR Experiments. In an oven-dried two-necked flask fitted with the IR probe (see above), **1** (2.0 mmol) was added to a stirring solution of toluene (8.0 mL) and 3 Å MSs (2.0 g, oven-dried at 250 °C for >48 h prior to use), under Ar at 25 °C. Once the C═O peak had plateaued, showing its maximal intensity, amine **2** (2.0 mmol) was added and the reaction was conducted for 0.5−24 h.

Standard Conditions for *in Situ* ^{1}H NMR Experiments. Enal or enone **1** (0.18 mmol) was added to an NMR tube (Norell Standard Series 5 mm × 178 mm NMR tubes) containing d_8-toluene (0.7 mL) with or without 3 Å MSs (filled 0.7−0.8 mm up the tube, MSs oven-dried at 250 °C for >48 h prior to use) that was flushed with argon and sealed. After the acquisition of the first spectrum, amine **2** (0.18 mmol) was added, and the next spectrum was acquired in <5 min. Subsequent ^{1}H NMR spectra were recorded over time with intermittent shaking of the NMR tube to aid mixing (see the Supporting Information).

dx.doi.org/10.1021/jo5007366 | J. Org. Chem. 2014, 79, 5163−5172

Computational Details. All calculations were performed using the Gaussian09 series of programs.[22] Full quantum mechanics calculations on model systems were performed within the framework of density functional theory (DFT) using the B3LYP functional.[23] The basis set for all the atoms was the 6-31G(d,p) basis set.[24] All geometry optimizations were full, with no restrictions using the Berny algorithm implemented in Gaussian09.[25] All minima and transition states were confirmed by performing frequency calculations. Transition states were characterized by a single imaginary frequency, whose normal mode corresponded to the expected motion. Because the qualitative trends on selectivity are not affected by the polarity of the solvent (see Tables 3 and 4), calculations were performed in vacuum. To confirm this reasoning, we computed the solvent effects of toluene and acetonitrile via the continuum IEF-PCM model[26] for the amine addition to the *s-trans* isomer of crotonaldehyde **1a**. After the effects of both solvents had been included, the energy differences between 1,2- and 1,4-addition pathways remained qualitatively and quantitatively similar to each other (+2.5 and +1.3 kcal mol^{-1} for toluene and acetonitrile, respectively) and to in vacuum calculations (i.e., +4.4 kcal mol^{-1}). The natural bond orbital (NBO) method[27] was used to analyze the resultant wave function in terms of optimally chosen localized orbitals, corresponding to a Lewis structure representation of chemical bonding. In the case of some *s-cis* transition states, the optimal Lewis structure was slightly modified to account for the second-order perturbative donor−acceptor interaction between the C_α lone pair and the $\pi^*_{C=O}$ orbital.

■ ASSOCIATED CONTENT

Supporting Information

General experimental details, ReactIR and NMR data, and DFT calculation data and geometries. This material is available free of charge via the Internet at http://pubs.acs.org.

■ AUTHOR INFORMATION

Corresponding Authors

*E-mail: j.carbo@urv.cat.

*E-mail: andy.whiting@durham.ac.uk.

Notes

The authors declare no competing financial interest.

■ ACKNOWLEDGMENTS

We thank the EPSRC for Doctoral Training Account funding to A.D.J.C., the Ministerio de Ciencia e Innovación (MICINN) of Spain (Projects CTQ2011-29054-C02-01 and CTQ2010-16226), and the Direcció General de Recerca (DGR) of the Autonomous Government of Catalonia (Grants 2009SGR462 and XRQTC).

■ REFERENCES

(1) (a) Perlmutter, P. *Conjugate Addition Reactions in Organic Synthesis*, 7th ed.; Tetrahedron Organic Chemistry; Pergamon: Oxford, U.K., 1992. (b) Rossiter, B. E.; Swingle, N. M. *Chem. Rev.* **1992**, *92*, 771. (c) Csáky, A. G.; de la Herrán, G.; Murcia, M. C. *Chem. Soc. Rev.* **2010**, *39*, 4080.

(2) For our previous work regarding the utilization of α,β-unsaturated imines in synthesis, see: (a) Fernández, E.; Gulyás, H.; Solé, C.; Whiting, A. *Adv. Synth. Catal.* **2011**, *353*, 376. (b) Fernández, E.; Gulyás, H.; Solé, C.; Mata, J. A.; Tatla, A.; Whiting, A. *Chem.—Eur. J.* **2011**, *17*, 14248. (c) Calow, A. D. J.; Batsanov, A. S.; Fernández, E.; Solé, C.; Whiting, A. *Chem. Commun.* **2012**, *48*, 11401. (d) Calow, A. D. J.; Solé, C.; Whiting, A.; Fernández, E. *ChemCatChem* **2013**, *5*, 2233. (e) Calow, A. D. J.; Batsanov, A.; Pujol, A.; Solé, C.; Fernández, E.; Whiting, A. *Org. Lett.* **2013**, *15*, 4810.

(3) (a) Osman, R.; Pardo, L.; Rabinowitz, J. R.; Weinstein, H. *J. Am. Chem. Soc.* **1993**, *115*, 8263. (b) Blackmond, D. G.; Hii, K. K.; Mathew, S. P.; Phua, P. H.; White, A. J. P.; de Vries, J. G. *Chem.—Eur. J.* **2007**, *13*, 4602. (c) Bernasconi, C. F. *Tetrahedron* **1989**, *45*, 4017.

(4) (a) Hine, J.; Via, F. A. *J. Am. Chem. Soc.* **1972**, *94*, 190. (b) Hine, J.; Craig, J. C., Jr.; Underwood, J. G., II; Via, F. A. *J. Am. Chem. Soc.* **1970**, *92*, 5194. (c) Chou, Y.; Hine, J. *J. Org. Chem.* **1981**, *46*, 649. (d) Smith, I. J. Ph.D. Thesis, Durham University, Durham, U.K., 2003. (e) Atherton, J. H.; Brown, K. H.; Crampton, M. R. *J. Chem. Soc., Perkin Trans. 2* **2000**, *5*, 941. (f) Sayer, J. M.; Jencks, W. P. *J. Am. Chem. Soc.* **1977**, *99*, 464. (g) Hoffman, R. V.; Bartsch, R. A.; Rae Cho, B. *Acc. Chem. Res.* **1989**, *22*, 211.

(5) (a) Ellman, J. A.; McMahon, J. P. *Org. Lett.* **2005**, *7*, 5393. (b) Bergman, R. G.; Colby, D. A.; Ellman, J. A. *J. Am. Chem. Soc.* **2006**, *128*, 5604. (c) Bergman, R. G.; Colby, D. A.; Ellman, J. A. *J. Am. Chem. Soc.* **2008**, *130*, 3645.

(6) (a) Cossío, F. P.; Odriozola, J. M.; Oiarbide, M.; Palomo, C. *J. Chem. Soc., Chem. Commun.* **1989**, 74. (b) Dembkowski, L.; Ganboa, I.; Kot, A.; Palomo, C. *J. Org. Chem.* **1998**, *63*, 6398. (c) Aizpurua, J. M.; Ganboa, I.; Oiarbide, M.; Palomo, C. *Eur. J. Org. Chem.* **1999**, 3223.

(7) Arndtsen, B. A.; Lu, Y. *Org. Lett.* **2009**, *11*, 1369.

(8) (a) Aparicio, D.; Palacious, F.; Vicario, J. *J. Org. Chem.* **2006**, *71*, 7690. (b) Palacios, F.; Pascual, S.; Ochoa de Retana, A. M.; Fernández de Trocóniz, G. *Tetrahedron* **2011**, *67*, 1575. (c) Ezpeleta, J. M.; Palacious, F.; Pascual, S.; Ochoa de Retana, A. M.; Fernández de Trocóniz, G. *Eur. J. Org. Chem.* **2013**, 5614.

(9) Alonso, C.; Ayerbe, M.; Cossío, F. P.; Lecea, B.; Palacios, F.; Rubiales, G. *J. Org. Chem.* **2006**, *71*, 2839.

(10) (a) Moyer, S. A.; Pearce, S. D.; Rigoli, J. W.; Schomaker, J. M. *Org. Biomol. Chem.* **2012**, *10*, 1746. (b) Soulé, J.-F.; Miyamura, H.; Kobayashi, S. *Chem. Commun.* **2013**, *49*, 355.

(11) Carter, C. F.; Lange, H.; Ley, S. V.; Baxendale, I. R.; Wittkamp, B.; Goode, J. G.; Gaunt, N. L. *Org. Process Res. Dev.* **2010**, *14*, 393.

(12) For information regarding additions to enones under kinetic or thermodynamic control, see: Schultz, A. G.; Yee, Y. K. *J. Org. Chem.* **1976**, *41*, 4044.

(13) Brown, K. H. Ph.D. Thesis, Durham University, Durham, U.K., 1999.

(14) (a) Benhallam, R.; Zair, T.; Jarid, A.; Ibrahim-Ouali, M. *J. Mol. Struct.: THEOCHEM* **2003**, *626*, 1. (b) Benhallam, R.; Essaoudi, A.; Zair, T. *Phys. Chem. News* **2002**, *8*, 110.

(15) See, for example: Romo, S.; Antonova, N. S.; Carbó, J. J.; Poblet, J. M. *Dalton Trans.* **2008**, 5166.

(16) (a) Barba, C.; Carmona, D.; García, J. I.; Lamata, M. P.; Mayoral, J. A.; Salvatella, L.; Viguri, F. *J. Org. Chem.* **2006**, *71*, 9831. (b) Loncharich, R. J.; Brown, F. K.; Houk, K. N. *J. Org. Chem.* **1989**, *54*, 1129.

(17) Bokareva, O. S.; Bataev, V. A.; Godunov, I. A. *J. Mol. Struct.: THEOCHEM* **2009**, *913*, 254.

(18) Durig, J. R.; Brown, S. C.; Kalasinsky, V. F.; George, W. O. *Spectrochim. Acta, Part A* **1976**, *32*, 807.

(19) (a) Fantoni, A. C.; Caminati, W. *Chem. Phys. Lett.* **1987**, *133*, 27. (b) During, J. R.; Little, T. S. *J. Chem. Phys.* **1981**, *75*, 3660. (c) Krantz, A. *J. Am. Chem. Soc.* **1972**, *94*, 4022.

(20) Feringa, B. L.; Jansen, J. F. G. A. *Synthesis* **1988**, *3*, 184.

(21) For an example of ReactIR being used to follow low-temperature lithiations, see: Campos, K. R.; Carbone, G.; Coldham, I.; O'Brien, P.; Sanderson, A.; Stead, D. *J. Am. Chem. Soc.* **2010**, *132*, 7260.

(22) Frisch, M. J.; Trucks, G. W.; Schlegel, H. B.; Scuseria, G. E.; Robb, M. A.; Cheeseman, J. R.; Scalmani, G.; Barone, V.; Mennucci, B.; Petersson, G. A.; Nakatsuji, H.; Caricato, M.; Li, X.; Hratchian, H. P.; Izmaylov, A. F.; Bloino, J.; Zheng, G.; Sonnenberg, J. L.; Hada, M.; Ehara, M.; Toyota, K.; Fukuda, R.; Hasegawa, J.; Ishida, M.; Nakajima, T.; Honda, Y.; Kitao, O.; Nakai, H.; Vreven, T.; Montgomery, J. A., Jr.; Peralta, J. E.; Ogliaro, F.; Bearpark, M.; Heyd, J. J.; Brothers, E.; Kudin, K. N.; Staroverov, V. N.; Kobayashi, R.; Normand, J.; Raghavachari, K.; Rendell, A.; Burant, J. C.; Iyengar, S. S.; Tomasi, J.; Cossi, M.; Rega, N.; Millam, J. M.; Klene, M.; Knox, J. E.; Cross, J. B.; Bakken, V.; Adamo, C.; Jaramillo, J.; Gomperts, R.; Stratmann, R. E.; Yazyev, O.; Austin, A. J.; Cammi, R.; Pomelli, C.; Ochterski, J. W.; Martin, R. L.;

Morokuma, K.; Zakrzewski, V. G.; Voth, G. A.; Salvador, P.; Dannenberg, J. J.; Dapprich, S.; Daniels, A. D.; Farkas, O.; Foresman, J. B.; Ortiz, J. V.; Cioslowski, J.; Fox, D. J. *Gaussian09*, revision A.02; Gaussian, Inc.: Wallingford, CT, 2009.
(23) (a) Lee, C.; Yang, W.; Parr, R. G. *Phys. Rev. B* **1988**, *37*, 785. (b) Becke, A. D. *J. Chem. Phys.* **1993**, *98*, 5648. (c) Stephens, P. J.; Devlin, F. J.; Chabalowski, C. F.; Frisch, M. J. *J. Phys. Chem.* **1994**, *98*, 11623.
(24) (a) Francl, M. M.; Pietro, W. J.; Hehre, W. J.; Binkley, J. S.; Gordon, M. S.; Defrees, D. J.; Pople, J. A. *J. Chem. Phys.* **1982**, *77*, 3654. (b) Hehre, W. J.; Ditchfield, R.; Pople, J. A. *J. Chem. Phys.* **1972**, *56*, 2257. (c) Hariharan, P. C.; Pople, J. A. *Theor. Chim. Acta* **1973**, *28*, 213.
(25) Pulay, P.; Fogarasi, G. *J. Chem. Phys.* **1992**, *96*, 2856.
(26) Mennucci, B.; Cancès, E.; Tomasi, J. *J. Phys. Chem. B* **1997**, *101*, 10506.
(27) Reed, A. E.; Curtiss, L. A.; Weinhold, F. *Chem. Rev.* **1988**, *88*, 889.